New passive microwave remote sensing technique for sea ice in the Sea of Okhotsk using 85-GHz channel of DMSP SSM/I

Kazutaka TATEYAMA[1], Hiroyuki ENOMOTO[1], Shuhei TAKAHASHI[1], Kazuyuki SHIRASAKI[1], Kinji HYAKUTAKE[1] and Fumihiko NISHIO[2]

[1] Department of Civil Engineering, Kitami Institute of Technology, Kitami, 090-8507, Japan
[2] Hokkaido University of Education, 1-15-55 Shiroyama, Kushiro, 085-8580, Japan

Abstract New sea ice classifying algorithm based on the 85-GHz channel of DMSP SSM/I is developed for the Sea of Okhotsk, and is based on aircraft measurements of the ice in the Lake Saroma and the Sea of Okhotsk by using a NASDA-developed airborne microwave radiometer (AMR), with the 89-GHz channels. This algorithm is applied to SSM/I data, and is calibrated by comparing to NOAA AVHRR and ADEOS AVNIR visible and near infrared data. The spatial resolution of ice area data derived from this algorithm increase to 4 times per pixel compare to the NASA team algorithm by using the 85-GHz channel which has the higher resolution, 12.5km than the other channels, 25km. Furthermore the false sea ice signals shown around the coast and marginal ice zone have decreased for all seasons by using this algorithm. This algorithm also attempts to classify sea ice types, fast ice, floes, young ice and new ice by using the difference between the dielectic properties of 85-GHz and 37-GHz channels on different sea ice types with the thickness.

1. Introduction

1.1 Sea ice in the Sea of Okhotsk

The sea ice in the Sea of Okhotsk, which is one of the lowest latitude ice pack area on the globe, consists entirely of first year ice. Observations by DMSP SSM/I that have been continuing since 1987, have shown that the fluctuations of concentration and extent of ice [*Nishio and Cho, 1996, Enomoto, 1996*], and a rapidly decrease of ice extent in the Sea of Okhotsk since 1989 [*Tachibana et al., 1996*]. However, in order to estimate the effect of global warming to sea ice, not only sea ice extent and concentration but also ice thickness should be analyzed because ice concentration might vary greatly due to the effect of wind.

In winter of 1996, field experiment for sea ice observation, called the Sea Ice Observation Program in the Sea of Okhotsk, was carried out using an airborne passive microwave multi-channel radiometer over the Lake Saroma and the eastern coast of Hokkaido. This report shows the results the development of a new algorithm based on the SIPSO experiment and applying the new algorithm to DMSP SSM/I data in whole the Sea of Okhotsk.

1.2. Sea ice remote sensing

Although algorithms calculating ice concentration, such as the NASA team [*Cavalieri et*

To be published in Bulletin of Glaciological research

al., 1991] algorithm and the Bootstrap algorithm [*Comiso et al, 1992*], are very useful tools in areas such as the Arctic and Antarctic, observation of sea ice in the Sea of Okhotsk involves some technical problems. The problems originate from false sea ice signals that come from atmospheric effects which turn up at low latitudes, and a coastal/land effect that contaminates the data due to the high ratio of land surrounding the sea [*Cho et al., 1996*].

Cavarieli (1994) presented a technique for mapping the distribution of new, young and first-year ice in the Bering Sea from SSM/I. This technique used the polarization ratio, which is sensitive to changes in ice thickness and ice surface characteristic, of 19-GHz and 37-GHz channels to classify. The polarization ratio varies with ice thickness from about 0.3 for open water, to about 0.15 for new ice, to 0.08 for young ice and to 0.03 for thick first-year ice. Although this technique has solved the problem, which thin ice signals regarded as multi-year ice in the seasonal ice areas, this technique still involves the problem, which is low resolution in local area and the confusion of concentration in the mixed ice types area.

The 85-GHz channels of SSM/I have a resolution of 12.5 km, twice the resolution of the other channels. However, the sea ice algorithms based on the DMSP SSM/I, the 19, 22 and 37-GHz, have been used for calculating ice concentration. Sea ice classification experiments that have been done by airborne sensors and in laboratories have also used the higher frequency channels [*Troy et al.,1981, Eppler et al., 1992*]. These experiments showed that distinction of ice types was possible by combining higher frequency channels with the other channels.

2. Study area and method

2.1 Test sites

The Sea of Okhotsk is located the area ranged from 44°N to 62°N, has an area of 1.5×10^6 km^2 (Fig. 1). This area used to freeze up to 80% until the 1980s, but since the 1990s the sea ice area has occupied only less than 60% [*Nishio and Cho, 1996, Tachbana et al., 1996*]. The Lake Saroma shown in Figure 1 is a salt lake connecting through two mouths to ocean and has an area of 150.4km^2. This lake freezes up in winter and this lake ice seems to be one stable huge floe. Therefore scientists have carried out safely several experiments of sea ice in this lake.

2.2. Aircraft measurements

Observations, using NASDA-developed Airborne Microwave Radiometer (AMR) mounted on the Beachcraft-200 (B-200), were carried out with the ground measurements in the Lake Saroma and the western coast of Hokkaido at 17th of February 1996. An airborne infrared radiometer was also used at 15th and 16th of February. AMR has 6 channels (Table 1), which

each have vertical and horizontal polarization. This instrument was developed for the ground experiment related to Advanced Microwave Scanning Radiometer (AMSR) for ADEOS-II Satellite, which will be launched in 2000. AMR data are relevant for comparison to SSM/I data due to cover over channels of SSM/I.

3. Results

In this study, the VTR images was taken from B-200 and used for the truth distribution data of the ice surface and thickness, because of the ice in the northwestern part was so thin that it was impossible to get the ground truth data in the whole lake.

The ice thickness distribution seemed to be different between the northwestern and southeastern. It was seen that the bare thin ice in the northwest, and it is getting thicker and much snow cover as going to the southwestward. In southwest, the mean ice thickness and the mean snow cover were approximately 30cm and 10cm respectively.

The general weather outlook was seen that air temperature increased close to 0 °C during 11th and 15th of February, and decreased rapidly to –18 °C at 16th of February. So that it is suppose to happen re-freezing on the ice surface in this period. At 17th of February, carried out AMR observation, air temperature had kept below –10 °C through the day, hence snow cover was seemed to be dry. Therefore it was supposed that the variation of the brightness temperature values derived from this experiment was related only to the variation of ice because the effect of snow cover might be taken as constant.

3.1 Sea ice signals

Figure 2 shows the distributions of brightness temperature, where ranged (a) from southeast to northwest (PATH-1) and (b) from land-side to ocean (PATH-2), received by each channels of AMR and the infrared radiometer. The spike-like noises seen on each horizontal polarized channels are supposed to be caused by interference from the outside electric waves.

It can be seen in the Figure 2 that variation is large in the horizontal polarization and it increases with high frequency, and the difference between both polarized channels decreases in the higher frequencies. The vertical polarized 89-GHz channel varies greatly for 30 K on ice and varies slightly on the open water.

Figure 2(a) indicates that the distribution of the 89-GHz channels signal varies with ice thickness and ice surface, from about 240 K on snow covered thick ice to about 270 K on thin bare ice. A feature of the 89-GHz channels is inferred to interact with the ice surface temperature because the variations are similar to the data obtained from infrared radiometer. In the other words, the 89-GHz channels are more sensitive even on the continuous ice than

the other channels and suppose to be reflect the difference of ice thickness and surface differences. Figure 2(b) shows significant decrease of brightness temperature on open water, but on the vertical polarized 89-GHz the variation is so small that it is difficult to distinguish open water signal.

3.2 Algorithm by using the 89-GHz

A parameter $R_{37V/89V}$ was established by the ratio between the vertically polarized 37-GHz (37V) and the vertically polarized 89-GHz (89V) of SSM/I, to obtain higher resolution ability than before and to discriminate ice types according to thickness. The $R_{37V/89V}$ is excepted to reflect the different radiometric properties between 37V and 89V and to express the difference of ice thickness on pack ice area, with concentration of 100%. So that when the $R_{37V/89V}$ indicates low value on pack ice area, the ice supposes to be low temperature, in the other words, to be thick. Conversely when the $R_{37V/89V}$ indicates high value, the ice supposes to be high temperature or to be thin. On the other hands, although 89V is not pertinent to differentiate open water in order to indicate almost same intensity to ice area, the $R_{37V/89V}$ is possible to discriminate clearly open water due to using 37V which is sensitive to the different between the ice and open water. This difference between 37V and 89V on open water is bigger than using 37V and the other channels, so that the $R_{37V/89V}$ is superior to find open water.

Figure 3 shows the results, which used the ice data consist of 100% concentration of new ice, young ice and floe, in the eastern coast of Hokkaido. Figure 3(a) used the NASA team algorithm (Cavarieli, 1991), Figure 3(b) used $R_{37V/89V}$ instead of GR(gradient ratio). GR and PR are given by,

$$GR_{37V/19V}=(T_{B37V}-T_{B19V})/(T_{B37V}+T_{B19V}) \quad (1)$$

$$PR_{19}=(T_{B19V}-T_{B19H})/(T_{B19V}+T_{B19H}) \quad (2).$$

The results show that it is hard to distinguish young ice from floe in terms of used the NASA team algorithm (Fig. 3(a)). On the other hand, when $R_{37V/89V}$ is used instead of GR, discriminations of the ice floe and young ice can be done by $R_{37V/89V}$=1.00 line (Fig. 3(b)). Young ice and new ice can be divided by $R_{37V/89V}$=0.92 and new ice and open water can be divided by $R_{37V/89V}$=0.86. The new ice, young ice, floe has a thickness less than 10cm, 10~30cm and more than 30cm, respectively. This algorithm used a parameter $R_{37V/89V}$ was named S/KIT (Sea ice Program in Sea of Okhotsk/Kitami Institute of Technology) algorithm. Table 2 summarizes the used $R_{37V/89V}$ values in this algorithm.

3.3 Applying to SSM/I data

The S/KIT algorithm was applied to SSM/I data in areas where the NASA team algorithm

showed ice concentrations of more than 80% and calibrated by using satellite visible and near-infrared data of AVHRR on NOAA. By referring the NASA-team algorithm, which has an ability to distinguish thin ice (Cavarieli, 1994), ice concentration(C) is calculated as a sum of concentration (C_A) of ice type A (first-year ice) and concentration (C_B) of ice type B (new ice), and is given by,

$$C_A=(a_0+a_1PR+a_2GR+a_3PR\cdot GR)/D \quad (3)$$

$$C_B=(b_0+b_1PR+b_2GR+b_3PR\cdot GR)/D \quad (4)$$

$$C=C_A+C_B \quad (5)$$

where,

$$D= c_0+c_1PR+c_2GR+c_3PR\cdot GR \quad (6).$$

The coefficient a_i, b_i, c_i (i=1, 2, 3) of the NASA team Algorithm was modified to use in the Sea of Okhotsk suggested by Enomoto (1996) as shown in Table 3. The weather filter is used if GR'>0.03 and GR> 0.05 then concentration is substituted for 0%, was selected. GR' is given by,

$$GR'=(T_{B22V}-T_{B19V})/(T_{B22V}+T_{B19V}) \quad (7).$$

Figure 4 shows a sample of sea ice map used the S/KIT algorithm (Fig. 4(c)) and compared with the concentration map used the modified the NASA team algorithm (the MNT algorithm) (Fig. 4(b)) and NOAA AVHRR image (Fig. 4(a)) at 30th of March 1996. The S/KIT algorithm was applied only in the concentrated ice area (>80% of ice concentration). Floe, young ice and open water are colored with purple, yellow and blue respectively. The threshold values of these areas, which show white, relative red and black on AVHRR image, were calibrated by comparing to AVHRR images, when the distinct difference between the both images is found. Shirasaki *et al.* (1998) observed thin ice area along the Sakhalin Is. using the ADEOS AVNIR data. Thin ice signal of S/KIT was checked along the Sakhalin using their results.

Fast ice, which looks like smooth surface and more bright white than floe around the estuary of the Amur River, is colored with red. The lower concentration area was indicated with a blue gradation, but their coverage is small. New ice is distinguished from young ice by using a parameter $R_{19H/85V}$. This parameter is using the horizontal polarized 19-GHz to find the ice, which shows relative low brightness temperature on this channel due to have most smooth surface such as nilas. New ice is colored with green. The calibrated threshold values of ice classification is summarized the specification of sea ice algorithm for Sea of Okhotsk.

3.4 Weather and Land Effect

It is necessary to remove the contamination originated from the atmosphere and the land in the Sea of Okhotsk due to more effective than the polar region. The contamination is suppose to happen in order to water vapor, clouds, rainfall and snowfall in terms of

atmosphere, and a false signal came from the side-lope of an antenna and a field of view ranged the land in the terms of land effect. It is possible to reduce the area affected from land noise by using the advanced resolution. This study applied the weather filter suggested by Comiso (1994) but slightly lower value. The concentration is set to be 0 when

$$T_{B22v}-T_{B19V} > 12 \qquad (7).$$

Figure 5 compares the seasonal march of ice extent in the Sea of Okhotsk calculated by the MNT algorithm and the S/KIT algorithm during January and December 1996. The ice extents are displayed by pixel unit, which equal to km^2 when multiplied by square of 12.5 km. There are no sea ice between June and beginning of November, thus ice signal in this duration is false signal. The false ice signals of the MNT algorithm in summer reach 10 % of mean ice extent in winter, but in terms of the S/KIT algorithm, that value is less than 3 % of that. It is found that the S/KIT algorithm has less the false ice signals than the MNT algorithm, with mean value 60 % and the maximum value 80 % in summer. Even in December and May, there could be a false signal due to land contamination. From this comparison, the S/KIT algorithm has more accuracy than the MNT algorithm because the resolution is advanced, hence the significant improvement was done for reducing the land contamination.

4. Concluding remarks

This study discussed possibility of improved sea ice algorithm based on the field experiments in Hokkaido, and comparisons with NOAA images. The higher frequency channels of 85 or 89-GHz are useful for detecting ice type and also improving the higher spatial resolution and less false ice signals than the MNT algorithm. NASDA satellite ADEOS-II will be launched in 2000. It mounted the Advanced Microwave Scanning Radiometer (AMSR), with 89-GHz channels. AMR has developed for the ground experiment of AMSR and has same channels to AMSR. Therefore the S/KIT algorithm based on AMR seems to be useful for AMSR data, is expected to offer the high resolution ice map with 5kmx5km since the 89-GHz channels of AMSR have 5km resolution.

We suggest following things;

· Development for a algorithm calculating ice concentration used the 85 or 89-GHz channels.

· Analyze the effect of the snow cover on the ice. Especially the behavior of brightness temperature in melting season should be analyzed due to the water content snow layer over ice will increase and affect greatly microwave radiation in this season.

· Apply the S/KIT algorithm to the other first-year ice area such as the Baltic Sea, the Bering Sea and the Barents Sea.

· Apply the S/KIT algorithm to multi-year ice area such as the Arctic and the Antarctic. In this

area, the ice from land such as iceshelf and iceberg also is needed to distinguish.

Acknowledgments

We used AMR data provided from the National Space Development Agency of Japan (NASDA), SSM/I data distributed from the National Snow and Ice Data Center (NSIDC).

References

Cavalieri, D. J., J. P. Crawford, M. R. Drinkwater, D. T. Eppler, L. D. Farmer, R. R. Jentz and C. C. Wackerman (1991): Aircraft Active and Passive Microwave Validation of Sea Ice Concentration From the Defense Meteorological Satellite Program Special Sensor Microwave Imager, J. Geophys. Res., **96**(C12), 21,989-22,008.

Cavalieri, D. J. (1994): A microwave technique for mapping thin ice, J. Geophys. Res., **99**(C6), 12,561-12,572.

Cho, K., N. Sasaki, H. Shimoda, T. Sakata, and F. Nishio (1996): Evaluation and improvement of SSM/I sea ice concentration algorithms for Sea of Okhotsk, Jour. Remote Sensing Society of Japan, **16**(2), 47-58.

Comiso, J. C., T. C. Grenfell, M. Lange, A. Lohanick, R. Moore, and P. Wadhams (1992): Microwave remote sensing of the Southern Ocean ice cover, Passive microwave signatures of sea ice, In Carsey, F.D. (ed.), Microwave remote sensing of sea ice, Gephys. Monogr, **68**, 47-71.

Comiso, J. C. (1994): Ice concentration derived using the bootstrap algorithm, NSIDC Letter attached to revised CD-ROM.

Comiso, J. C., D. J. Cavalieri, C. L. Parkinson and P. Gloersen (1997): Passive Microwave Algorithms for Sea Ice Concentration: A Comparison of Two Techniques, Remote Sens. Environ., **60**, 357-384.

Enomoto, H. (1996): Observation of thin ice area in the Okhotsk Sea and impacts for climatological study, Jour. Remote Sensing Society of Japan, **16**(2), 14-25.

Eppler D.T., L. D. Farmer, A. W. Lohanick, M. R. Anderson, D. J. Cavalieri, J. Comiso, P. Gloersen, C. Garrity, T. C. Grenfell, M. Hallikainen, J. A. Maslanik, C. Matzler, R. A. Melloh, I. Rubinstein and C. T. Swift (1992): Passive microwave signatures of sea ice, In Carsey, F.D. (ed.), Microwave remote sensing of sea ice, Gephys. Monogr, **68**, 47-71.

Nishio, F. and K. Cho (1996): Sea ice extents in the Okhotsk Sea -improvement for sea ice concentration and climatic interpretation, Jour. Remote Sensing Society of Japan, **16**(2), 26-31, 1996.

Shirasaki, K., H. Enomoto, K. Tateyama, H. Warashina and A. Watanabe (1998):Observation of sea ice conditions using visible and near-infrared channels in MOS-1/MESSR and ADEOS/AVNIR, Polar Meteol. Glaciol., **12**, 86-96.

Tachibana, Y., M. Honda and K. Takeuchi (1996): The abrupt decrease of the sea ice over the southern part of the Sea of Okhotsk in 1989 and its relation to the recent weakening of the Aleutian low, J. Meteorol. Soc. Japan, **74**(4), 579-584.

Troy, B. E., J. P. Hollinger, R. M. Lerner and M. M. Wisler (1981): Measurement of the Microwave Properties of Sea Ice at 90 GHz and Lower Frequencies, J. Geophys. Res., **86**(C5), 4283-4289.

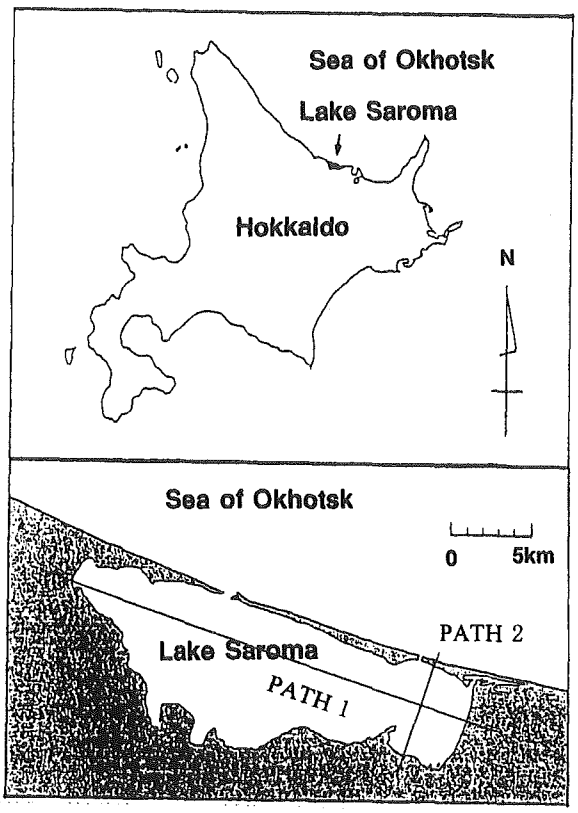

Fig. 1. Location of the Sea of Okhotsk and Lake Saroma

Table 1. The channels of SSM/I, AMR and AMSR

Sensor	Channels (GHz) / Resolution (km)					
SSM/I			19.35	22.23	37.0	85.5
			25			12.5
AMSR	6.9	10.65	18.7	23.8	36.5	89.0
	50		25		15	5
AMR	6.9	10.65	18.7	23.8	36.5	89.0

Table 2. Threshold values of 85 and 37 GHz Ratio for four ice types, lower concentration area than 80% and open water.

Categories	Threshold Values
Fast Ice	$1.12 < R_{37V/85V}$
Floe	$1.00 < R_{37V/85V} < 1.12$
Young Ice	$0.97 < R_{37V/85V} < 1.00$
Newly Formed Ice	$0.92 < R_{37V/85V} < 0.97$
	$0.20 < R_{19H/85V} < 0.30$
Low Concentration	$0.92 < R_{37V/85V} < 0.97$
Open Water	$R_{37V/85V} < 0.92$

Table 3. The modified coefficients of the NASA team algorithm (Enomoto, 1996)

Coefficients		
a_0= 1255	b_0= 687	c_0=-721
a_1=-10996	b_1= 600	c_1= 12936
a_2= 18679	b_2= 3417	c_2=-31260
a_3= 30929	b_3= 3504	c_3=-44918

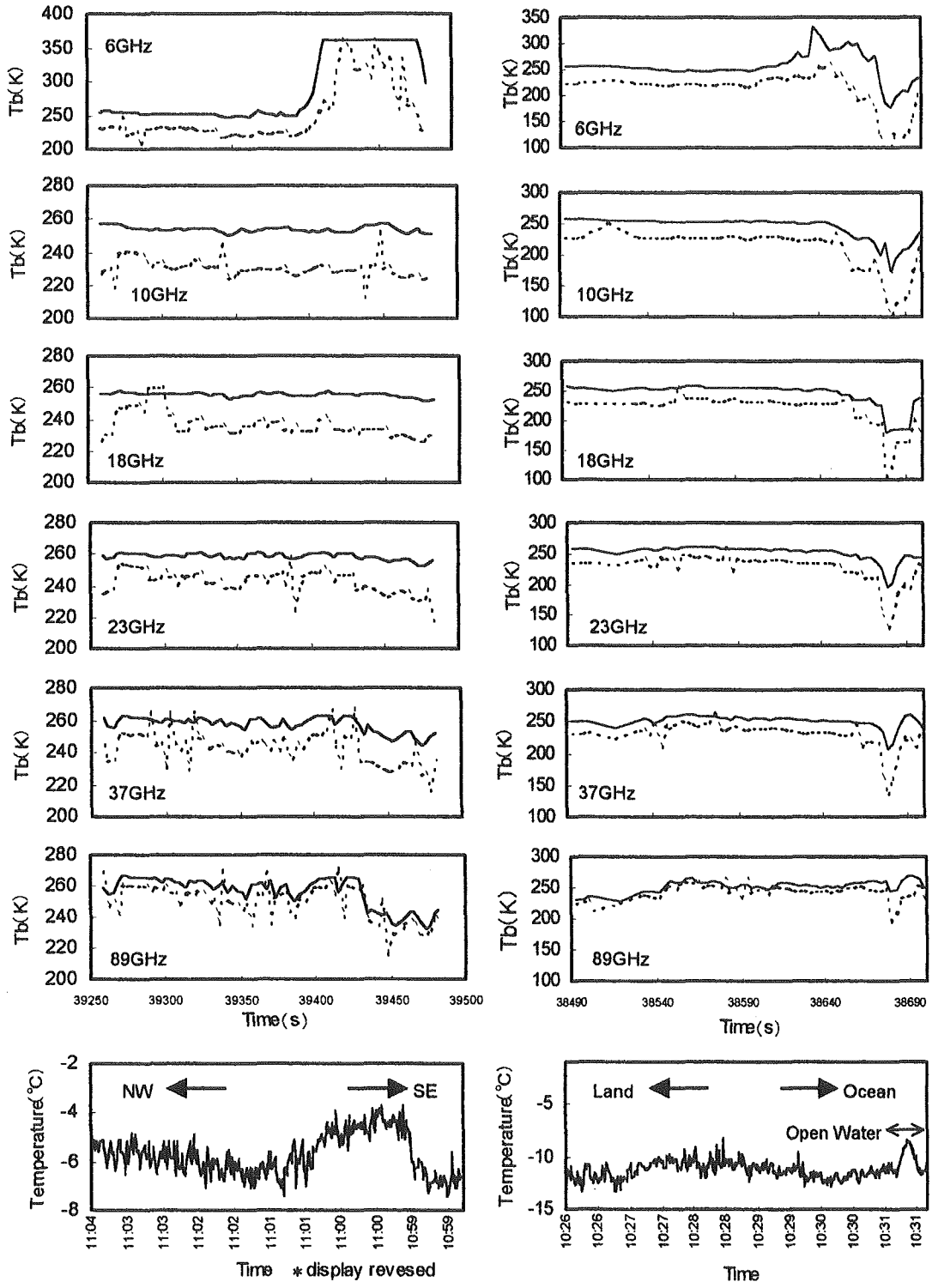

(a) PATH-1 (b) PATH-2

Fig.2. The distribution of AMR (V-pol: solid line, H-pol.: dashed line) at 17th of February and infrared radiometer data

(a) PATH-1 (SE-NW), infrared data was taken at 15th of February

(b) PATH-2 (from land to ocean), infrared data was taken at 16th of February.

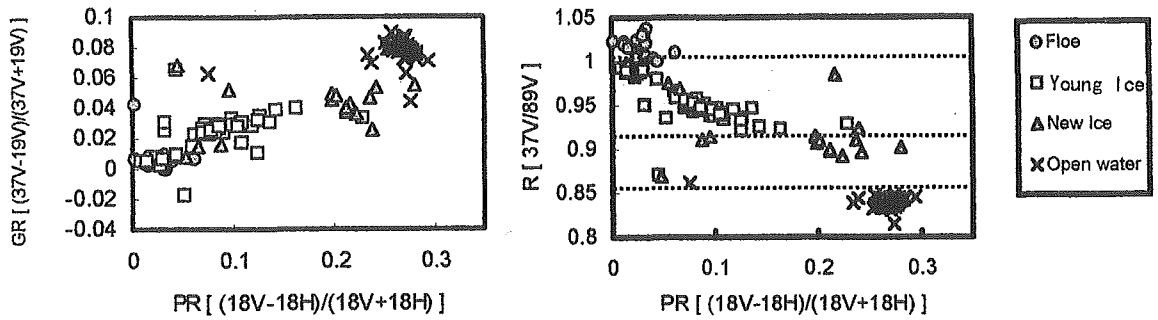

(a) The NASA team algorithm (b) used $R_{37V/89V}$ instead of GR

Fig.3. (a) Ice signals distribution in the Sea of Okhotsk used NASA team Algorithm
(b) Ice signals distribution in the Sea of Okhotsk used $R_{37V/89V}$ parameter

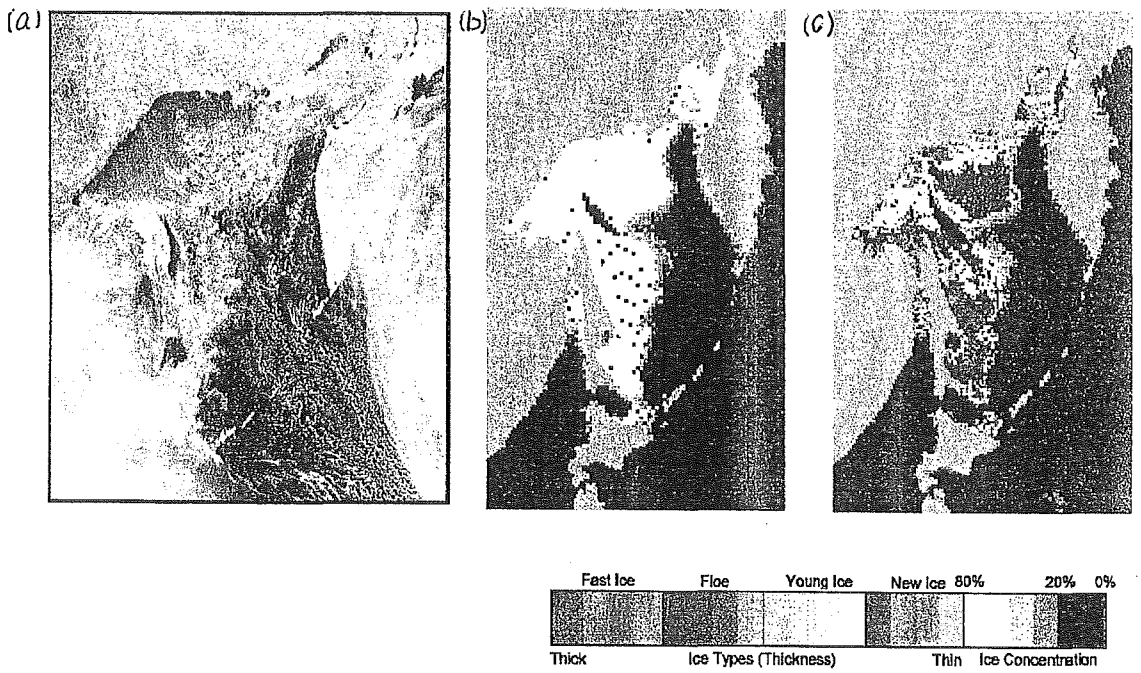

Fig. 4. Satellite Images at 30th of March 1996.
(a) NOAA AVHRR image,
(b) sea ice concentration map by the NASA team algorithm (white: concentration>80%),
(c) sea ice map by the S/KIT algorithm (color scale: ice type).

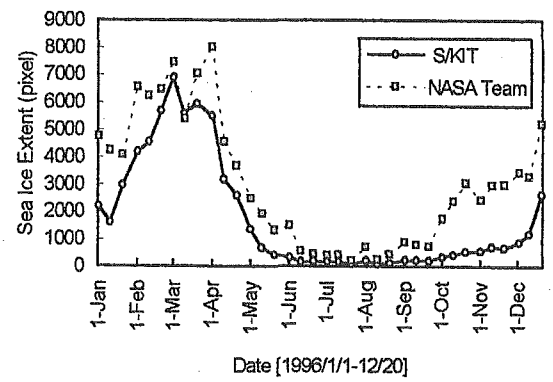

Fig. 5. A time series of sea ice extent. the solid line shows the S/KIT algorithm and the dashed line shows the NASA team algorithm.